Figure S1

A

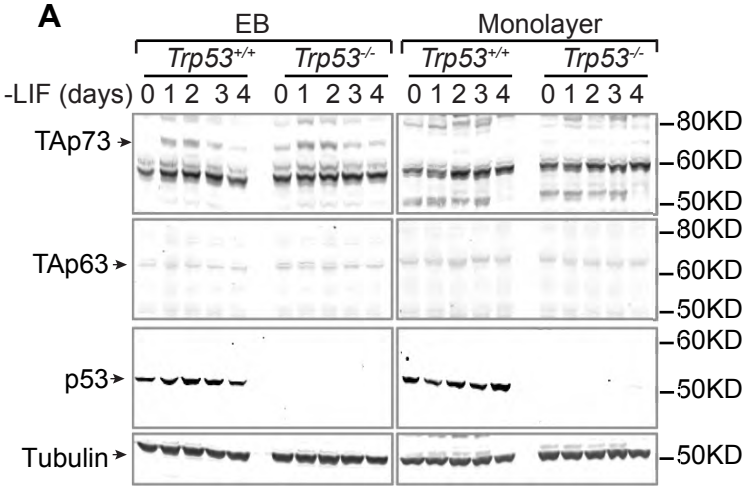

B

mRNA level of p53 family member (RPM)

-LIF(Days)	D0	D1	D2	D3	D4
Trp53	432.17	549.29	330.37	260.36	299.97
Trp63	0.07	0.18	0.08	0.14	0.16
Trp73	15.78	26.88	29.87	17.77	5.72
Gapdh	150.60	159.20	219.83	256.60	191.32

C

p53/p63/p73 knockout by CRISPR/Cas9

Trp53$^{+/+}$;*Trp63*$^{+/+}$;*Trp73*$^{+/+}$ (WT) mESC

↓ *Trp63* exon4 sgRNAs, *Trp73* exon4 sgRNAs

Trp53$^{+/+}$;*Trp63*$^{-/-}$;*Trp73*$^{-/-}$ (DKO) clone

↓ *Trp53* exon4 sgRNAs

Trp53$^{-/-}$;*Trp63*$^{-/-}$;*Trp73*$^{-/-}$ (TKO) clones #1 & 2

D

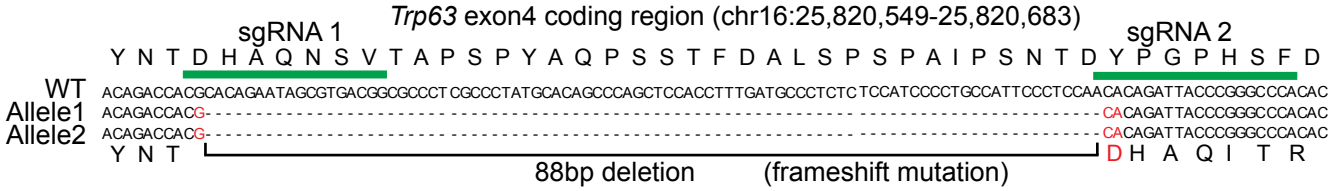

E

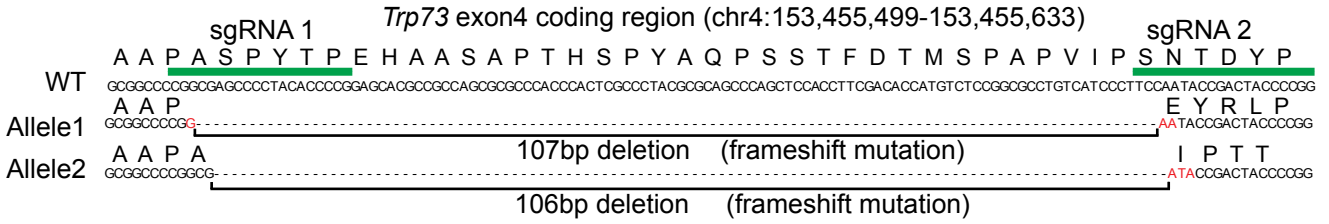

F

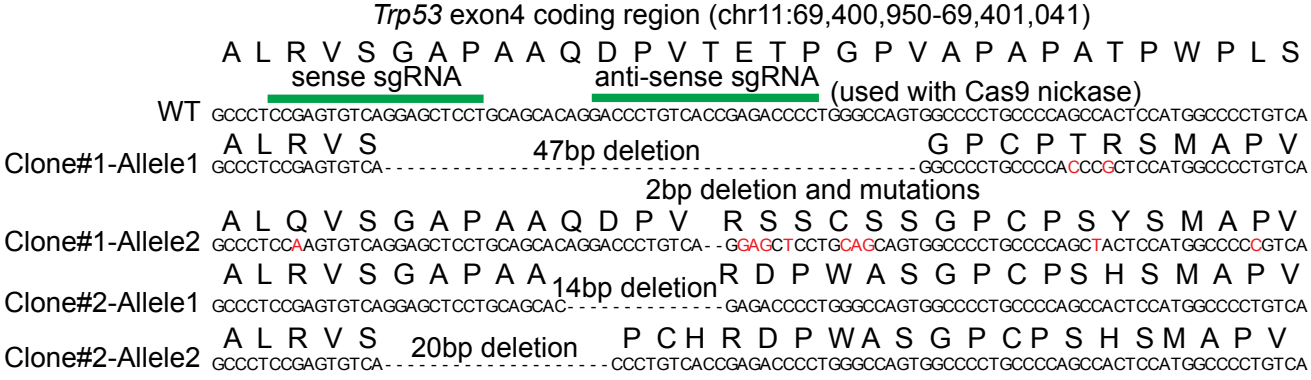

G

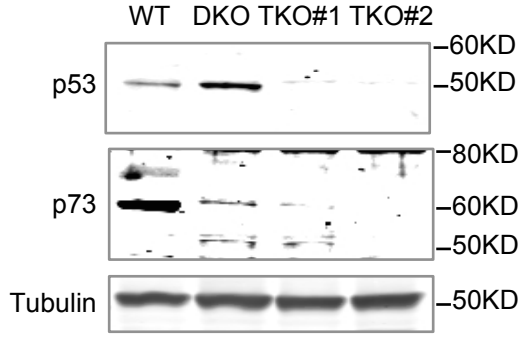

H

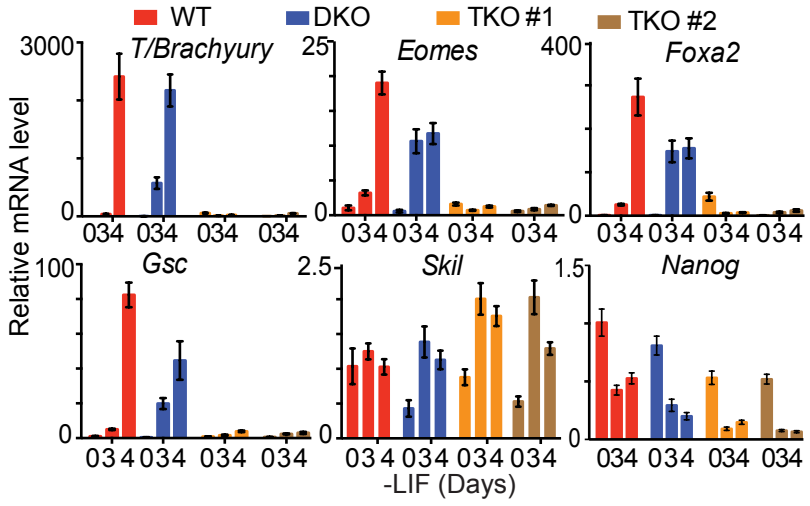

Figure S2

A

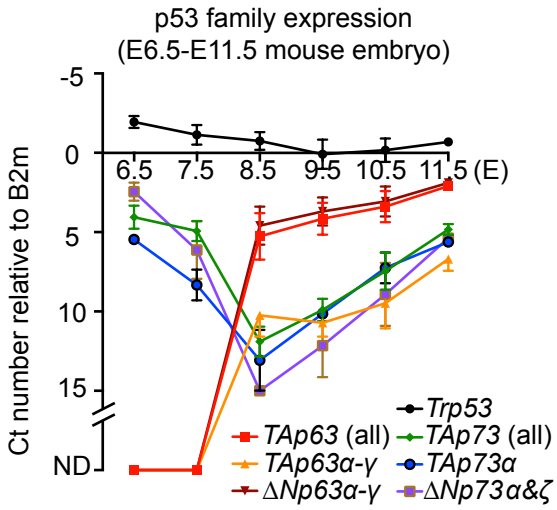

B

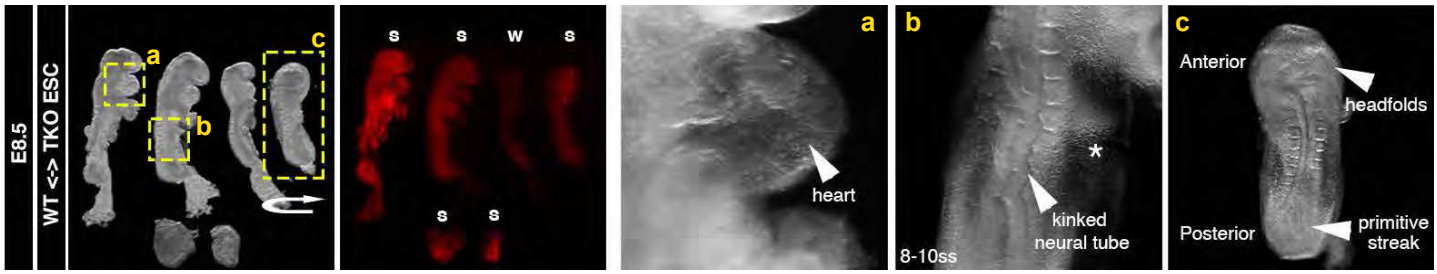

C

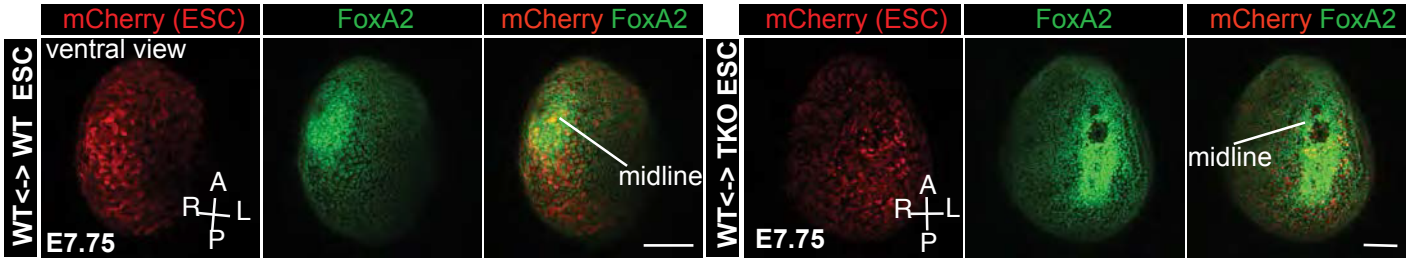

Figure S3

A

Motif enrichment in p53 ChIP-Seq: EB-AC		
Motif	**factor**	**logP-value**
	p53/p63/p73	-3.111e+03
	Tcfcp2l1	-5.590e+01

B

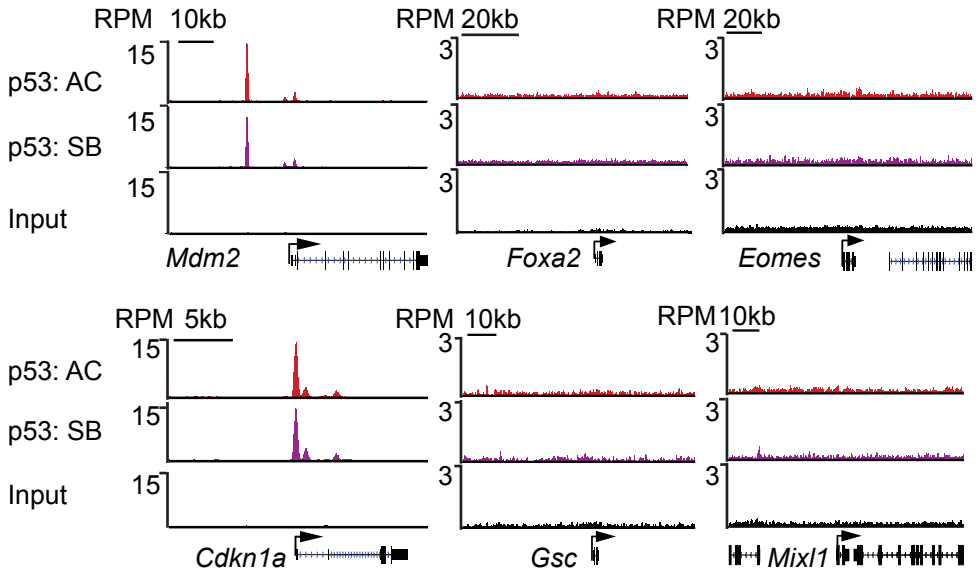

C

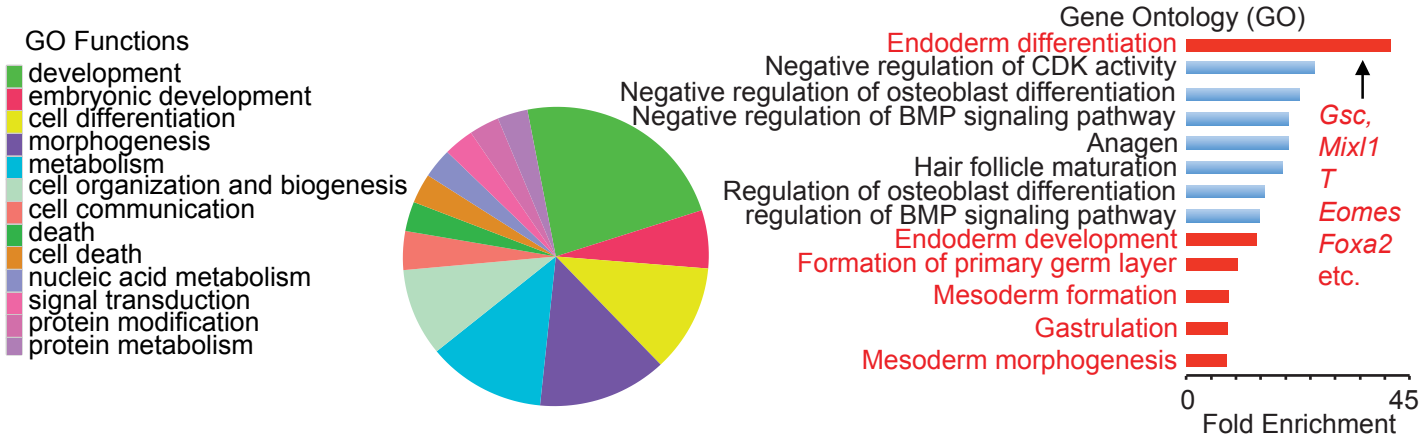

Figure S4

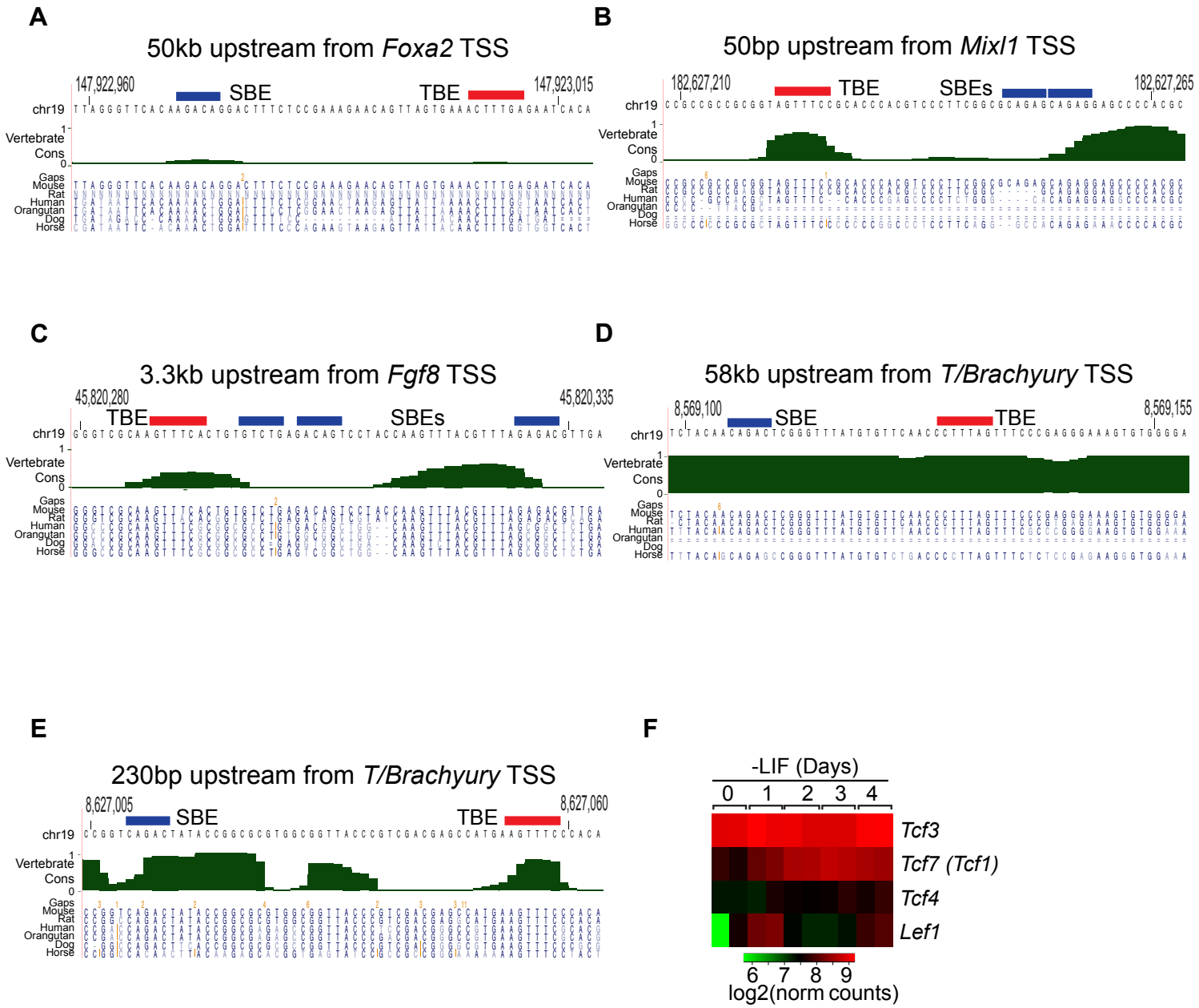
A
50kb upstream from *Foxa2* TSS
147,922,960
SBE
TBE
147,923,015
chr19
Vertebrate Cons
Gaps
Mouse
Rat
Human
Orangutan
Dog
Horse
B
50bp upstream from *Mixl1* TSS
182,627,210
TBE
SBEs
182,627,265
C
3.3kb upstream from *Fgf8* TSS
45,820,280
TBE
SBEs
45,820,335
D
58kb upstream from *T/Brachyury* TSS
8,569,100
SBE
TBE
8,569,155
E
230bp upstream from *T/Brachyury* TSS
8,627,005
SBE
TBE
8,627,060
F
-LIF (Days)
0 1 2 3 4
Tcf3
Tcf7 (Tcf1)
Tcf4
Lef1
6 7 8 9
log2(norm counts)

Figure S5

A

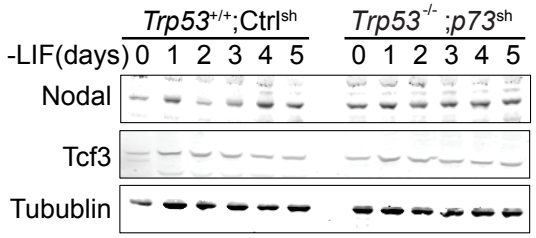

B

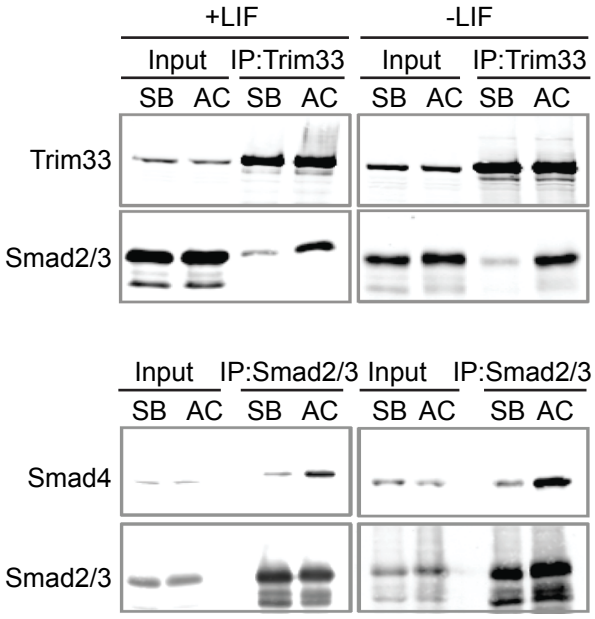

C

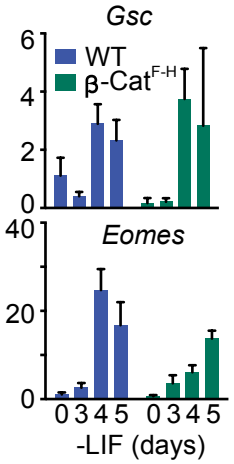

Figure S6

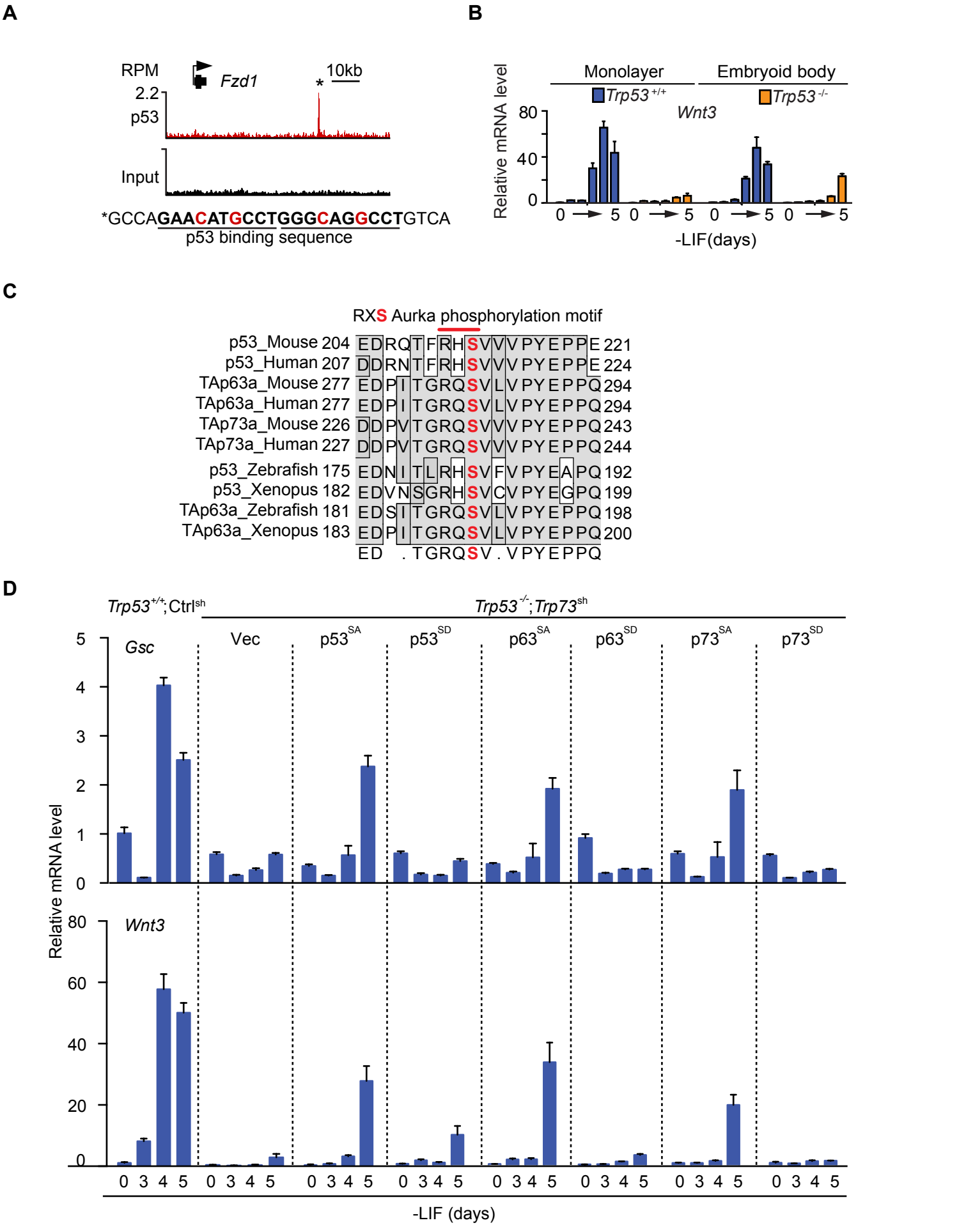
A
RPM
2.2
p53
Fzd1
10kb
Input
*GCCAGAACATGCCTGGGCAGGCCTGTCA
p53 binding sequence
B
Monolayer
Embryoid body
Trp53+/+
Trp53-/-
Wnt3
Relative mRNA level
80
40
0
0 → 5 0 → 5 0 → 5 0 → 5
-LIF(days)
C
RXS Aurka phosphorylation motif
p53_Mouse 204 EDRQTFRHSVVVPYEPPE 221
p53_Human 207 DDRNTFRHSVVVPYEPPE 224
TAp63a_Mouse 277 EDPITGRQSVLVPYEPPQ 294
TAp63a_Human 277 EDPITGRQSVLVPYEPPQ 294
TAp73a_Mouse 226 DDPVTGRQSVVVPYEPPQ 243
TAp73a_Human 227 DDPVTGRQSVVVPYEPPQ 244
p53_Zebrafish 175 EDNITLRHSVFVPYEAPQ 192
p53_Xenopus 182 EDVNSGRHSVCVPYEGPQ 199
TAp63a_Zebrafish 181 EDSITGRQSVLVPYEPPQ 198
TAp63a_Xenopus 183 EDPITGRQSVLVPYEPPQ 200
ED . TGRQSV . VPYEPPQ
D
Trp53+/+;Ctrlsh
Trp53-/-;Trp73sh
Vec
p53SA
p53SD
p63SA
p63SD
p73SA
p73SD
Gsc
Wnt3
Relative mRNA level
0 3 4 5
-LIF (days)

Figure S7

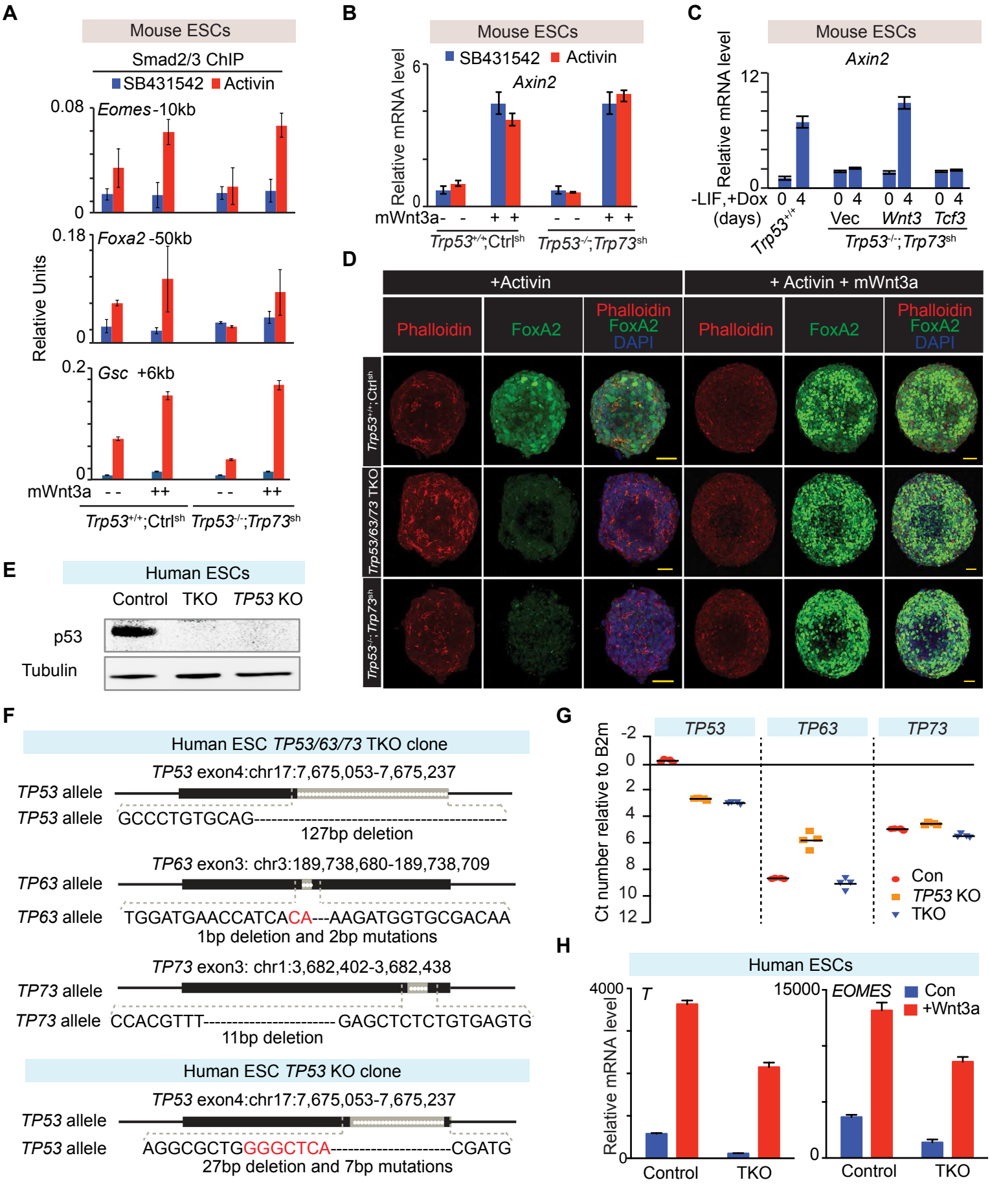
A
Mouse ESCs
Smad2/3 ChIP
SB431542 Activin
Eomes -10kb
Foxa2 -50kb
Gsc +6kb
Relative Units
mWnt3a - - ++ - - ++
Trp53+/+;Ctrlsh
Trp53-/-;Trp73sh
B
Mouse ESCs
SB431542 Activin
Axin2
Relative mRNA level
mWnt3a- - + + - - + +
Trp53+/+;Ctrlsh
Trp53-/-;Trp73sh
C
Mouse ESCs
Axin2
Relative mRNA level
-LIF,+Dox (days) 0 4 0 4 0 4 0 4
Trp53+/+
Vec Wnt3 Tcf3
Trp53-/-;Trp73sh
D
+Activin
+ Activin + mWnt3a
Phalloidin
FoxA2
Phalloidin FoxA2 DAPI
Trp53+/+;Ctrlsh
Trp53/63/73 TKO
Trp53-/-;Trp73sh
E
Human ESCs
Control TKO TP53 KO
p53
Tubulin
F
Human ESC TP53/63/73 TKO clone
TP53 exon4:chr17:7,675,053-7,675,237
TP53 allele
TP53 allele GCCCTGTGCAG----------
127bp deletion
TP63 exon3: chr3:189,738,680-189,738,709
TP63 allele
TP63 allele TGGATGAACCATCACA---AAGATGGTGCGACAA
1bp deletion and 2bp mutations
TP73 exon3: chr1:3,682,402-3,682,438
TP73 allele
TP73 allele CCACGTTT---------- GAGCTCTCTGTGAGTG
11bp deletion
Human ESC TP53 KO clone
TP53 exon4:chr17:7,675,053-7,675,237
TP53 allele
TP53 allele AGGCGCTGGGGCTCA----------CGATG
27bp deletion and 7bp mutations
G
TP53
TP63
TP73
Ct number relative to B2m
Con
TP53 KO
TKO
H
Human ESCs
T
EOMES
Con
+Wnt3a
Relative mRNA level
Control TKO
Control TKO

SUPPLEMENTAL FIGURE LEGENDS

Supplemental Figure 1. The p53/p63/p73 family redundantly regulates ES cell mesendoderm differentiation. Related to Figure 1.

A. Western immunoblot analysis for p53, p63 and p73 protein levels in *Trp53*$^{+/+}$ or *Trp53*$^{-/-}$ cells over 4 days in EB or monolayer differentiation conditions. Tubulin was used as loading control. Experiments were performed in triplicate and representative results are presented.

B. mRNA expression levels (RNA-Seq) of *Trp53*, *Trp63*, *Trp73* and *Gapdh* in d0 to d4 EBs. Read counts were normalized to reads per million reads (RPM). Mean counts of two biological replicates are presented.

C. Scheme for the strategy of CRISPR-mediated *Trp53/Trp63/Trp73* knockout.

D-E. CRISPR sgRNA sequences and the genomic sequences of *Trp63* exon4 locus (D) and *Trp73* exon4 locus (E) in mutant clones DKO, TKO#1 and TKO#2.

F. CRISPR sgRNA sequences and the genomic sequences of *Trp53* exon4 locus in mutant clones TKO#1 and TKO#2.

G. Western immunoblot analysis for p53 and p73 in wild type (WT) or mutant clones (DKO, TKO#1, TKO#2) under pluripotent conditions. Tubulin was used as loading control.

H. mRNA expression analysis (qRT-PCR) of mesendoderm marker genes *T/Brachyury*, *Eomes*, *Foxa2*, *Gsc*, nodal feedback gene *Skil*, and pluripotency-associated gene *Nanog* in WT, DKO, and TKO#1 and #2 cells during EB differentiation. Error bars represent s.e.m.

Supplemental Figure 2. Loss of p53/p63/p73 leads to early embryonic defects in mouse development. Related to Figure 2.

A. mRNA expression levels (qRT-PCR) of p53 family isoforms in E6.5-E11.5 mouse embryos. Y-axis represents qPCR Delta Ct number relative to *B2m*. *n*=3. ND: not detectable, level below the sensitivity limit of qPCR.

B. Bright field and red fluorescence (mCherry) images of embryo chimeras comprising *Trp53*$^{-/-}$;*Trp63*$^{-/-}$;*Trp73*$^{-/-}$ triple KO (TKO) ES cells dissected at E8.5. Panels on the right (a, b, c) depict high magnification bright field images highlighting developmental delay and aberrant morphology, including defects in the heart and neural tube. Level of chimerism is categorized as strong (s) or weak (w). Arrowheads, related embryonic structures.

C. 3D reconstructed views of whole mount embryo chimeras comprising control (WT) or TKO ES cells dissected at E7.75 and imaged for mCherry (*red*, ES cell descendants) and FoxA2 expression (*green*). TKO ES cell chimeras exhibit an interrupted midline (middle row), which is consistent with a defect at gastrulation. Note that the unaffected FoxA2-positive cell population on the embryo's surface is visceral endoderm, which is not pluripotent epiblast-derived. Scale bars: 100 μm

Supplemental Figure 3. The p53 family selectively enables Smad2/3 binding to mesendoderm genes. Related to Figure 3.

A. Enriched transcription factor binding motifs in p53 bound regions in day-3 EBs treated with Activin A for 2h.

B. Gene track view for p53 ChIP-Seq data or input control at the *Mdm2*, *Cdkn1a* ($p21^{Cip}$), *Foxa2*, *Eomes*, *Gsc* and *Mixl1* loci. Day-3 EBs were treated with SB431542 (SB) or Activin A (AC) for 2 h. Gene bodies are schematically represented at the bottom of each track set.

C. Gene Ontology analysis for genes adjacent to p53/p73-dependent Smad2/3 ChIP-Seq peaks. Examples of genes included in Gene Ontology term "Endoderm Differentiation" are highlighted.

Supplemental Figure 4. Tcf factors cooperate with Smad2/3 to activate mesendoderm gene enhancers. Related to Figure 4.

A–E. Evolutionary conservation (Vertebrate Conservation Score) and genomic sequence alignments of regions that are 50kb upstream from *Foxa2* transcription start site (TSS) (A), 50bp upstream from *Mixl1* TSS (B), 3.3kb upstream from *Fgf8* TSS (C), 58kb upstream from *T/Brachyury* TSS (D) and 230bp upstream from *T/Brachyury* TSS (E).

F. Heatmap of Tcf family members *Tcf3, Tcf7* (*Tcf1*)*, Tcf4, Lef1* mRNA expression levels (RNA-Seq) from d0 to d4 of EB differentiation. Scale represents the log2 normalized read counts.

Supplemental Figure 5. Wnt family regulates Tcf3/Smad2/3 activity through β-catenin activation. Related to Figure 5.

A. Western immunoblot analysis of Nodal and Tcf3 in control ($Trp53^{+/+}$;$Ctrl^{sh}$) and p53/p73-depleted ($Trp53^{-/-}$;$Trp73^{sh}$) cells over 5 days under EB differentiation conditions. Tubulin (Tub) was used as loading control.

B. Western immunoblot analysis of Activin-induced complexes for the immunoprecipitation between Smad2/3, Smad4 and Trim33 in ES (+LIF) and day-3 EB (-LIF) cells. Cells were treated with Activin A (AC) or SB431542 (SB) for 2 h. 2% input was used as control.

C. *Gsc* and *Eomes* mRNA levels (qRT-PCR) in EBs derived from wild type (WT) or $\beta\text{-}Cat^{F\text{-}H}$ cell lines.

Supplemental Figure 6. The p53 family directly regulates Wnt3 expression for mesendoderm differentiation. Related to Figure 6.

A. Gene track view for p53 ChIP-Seq data or input control at the *Fzd1* locus. RefSeq gene body for *Fzd1* is schematically represented at the top of tracks. Asterisk (*) marks the p53-binding site at the putative *Fzd1* enhancer. Genomic sequence for the center of this site is listed at the bottom and the p53 consensus binding sequence is highlighted.

B. mRNA expression analysis (qRT-PCR) of *Wnt3* in the $Trp53^{+/+}$ or $Trp53^{-/-}$ cells under EB or monolayer conditions.

C. qRT-PCR analysis of *Wnt3* mRNA expression in EBs derived from $Trp53^{+/+}$;$Ctrl^{sh}$ and $Trp53^{-/-}$;$Trp73^{sh}$ ES cells at indicated time points.

D. Amino acid sequence alignment for p53/TAp63/TAp73 proteins from representative vertebrates: zebrafish, *Xenopus*, mouse and human. Red line, conserved R(H/Q)S Aurka phosphorylation motif. Ser212 p53 and the corresponding residues in other family members are marked in red and bold.

E. mRNA expression analysis (qRT-PCR) of *Gsc* and *Wnt3* in EBs derived from indicated ES cell lines. Error bars represent s.e.m. Vec: empty vector. SA: Ser to Ala mutation, SD: Ser to Asp mutation.

Supplemental Figure 7. Wnt3 mediates p53 family action in mesendoderm specification. Related to Figure 7.

A. ChIP-qPCR analysis for Smad2/3 binding to the *Eomes* -10kb, *Foxa2* -50kb and *Gsc* +6kb enhancers in control ES cells ($Trp53^{+/+}$;$Ctrl^{sh}$), or p53/p73-depleted cells ($Trp53^{-/-}$;$Trp73^{sh}$) treated with PBS or

recombinant mouse Wnt3a (mWnt3a), followed by addition of SB431542 or activin for 2 h. Error bars represent s.e.m.

B. mRNA expression analysis (qRT-PCR) of *Axin2* in control (*Trp53*$^{+/+}$;Ctrl^{sh}) and p53/p73-depleted (*Trp53*$^{-/-}$;*Trp73*^{sh}) cells, that were treated with or without recombinant mouse Wnt3a (mWnt3a) for 24h, followed by addition of SB431542 or Activin A for 2 h. Error bars represent s.e.m.

C. mRNA expression analysis (qRT-PCR) of *Axin2* in control (*Trp53*$^{+/+}$;Ctrl^{sh}) and p53/p73-depleted (*Trp53*$^{-/-}$;*Trp73*^{sh}) cells constructed with doxycycline (Dox)-inducible expression of *Wnt3*, *Tcf3* or empty vector (Vec). Assays were performed at d0 or d4 of Dox treatment under differentiation conditions. Error bars represent s.e.m.

D. Immunofluorescence analysis of FoxA2 (*green*) expression in d3 EBs derived from the indicated ES cell lines. Cells are treated with Activin A for 20h or Activin A with mWnt3a for 20h. Scale bar of each figure represents 50*μm*. Phalloidin (Carney et al.)(*red*) was used to stain F-actin and mark cell boundaries.

E. Western immunoblot analysis of p53 in wild type H1 cells (Control) or mutant clones (TKO and *TP53*KO) under pluripotency conditions. Tubulin was used as a loading control.

F. Human *TP53/63/73* TKO and *TP53* KO clone sequence of *TP53* exon4 locus, *TP63 and TP73* exon3 loci.

G. mRNA expression levels (qRT-PCR) of p53 family isoforms in H1 hESCs. Y-axis represents qPCR Delta Ct number relative to *B2microglobulin*.

H. qRT-PCR analysis of the indicated mRNA levels in control H1 hESCs or *TP53/63/73* TKO cells that were treated with or without recombinant Wnt3a for 24h,

SUPPLEMENTAL EXPERIMENTAL PROCEDURES

Cell line maintenance and differentiation

E14Tg2a.IV mouse ES cells were maintained on gelatin (0.1%, Millipore, ES-006-B) coated plates in LIF-supplemented medium at 37°C with 5% CO_2 (Xi et al., 2011). Basic ES cell medium included 80% Knockout DMEM (Life Technologies, 10829-018), 15% Fetal Bovine Serum (HyClone, SH30071), 50U Penicillin and 50ug/ml Streptomycin (Cellgro, 30-001-CI), 1% Non-essential Amino acids (Life Technologies, 11140-050), 1% L-Glutamine (Life Technologies, 25030081), 100μM β-Mercaptoethanol (Sigma-Aldrich, M6250), 10^3 U/ml mouse LIF (Gemini Bio-Products, 400-495). Mouse ESCs *Trp53*$^{+/+}$ and *Trp53*$^{-/-}$ cell lines were kindly provided by Jing Huang (Li et al., 2012) and maintained in N2B27 LIF+2i (PD0325901, 1μM, Cayman; CHIR99021, 3 μM, Cayman) (Ying et al., 2008) medium. Mouse EB formation and differentiation were carried out as described by ATCC.

In order to promote hESC mesendoderm differentiation, we differentiated H1 control and mutant cells in serum-free STEMdiff Apel Medium (Stem Cell Technologies #05210) as spin embryoid bodies (EBs) (Ng et al., 2008). Briefly, $3x10^3$ cells were seeded per well of a 96-well round-bottom untreated microplate (Corning #3788) in APEL Medium supplemented with 100ng/ml Activin A (Peprotech #120-14E), 20ng/ml BMP4 (R&D, 314-BP-010) and 10uM Y-27632 ROCK Inhibitor (Selleck Chemicals #1049) (Soh et al., 2014). H1 control cells were also supplemented with the WNT antagonist IWP-2 (Tocris Bioscience #3533). Cells were aggregated by centrifugation at 300 x *g* for 5mins and EBs were collected for RNA extraction.

CRISPR primers

For mouse ESCs, sgRNA target sequences are as following: *Trp53* exon4 Cas9n sgRNA sense strand: ACCCTGTCACCGAGACCCC, anti-sense strand: AGGAGCTCCTGACACTCGG; *Trp63* exon4 sgRNA 1: CCGTCACGCTATTCTGTGCG; sgRNA 2; TGGGCCCGGGTAATCTGTGT; *Trp73* exon4 sgRNA 1, CGGGGTGTAGGGGCTCGCCG; sgRNA 2: CCGGGGTAGTCGGTATTGGA; *Eomes* -10kb enhancer sgRNA 1: TAACAGTATTAACATCCCGC, sgRNA 2: CTCTCCGCTTTGATGTGAGC; *Gsc* +6kb enhancer sgRNA1: CAGCACAGACTGTGTCCTG, sgRNA 2: CAGACCATGTTTTCAAAGC; *Ctnnb1* (β-catenin) Cas9n sgRNA sense strand: AGTAGCCATTGTCCACGCAG, anti-sense strand: GTGATTCAGATGCCTGTCTG; FLAG-HA epitope tag oligo DNA template for *Ctnnb1*: CTTAAGTTTTAATGACTTGATGGAATTTTTCAGGGTACCTGAAGCTCAGCGCACAGCTGCTGTGACACC GCTGCGTGGACAATGGACTACAAAGACGATGACGACAAGGCCGCATACCCATACGATGTTCCAGATT ACGCTGCTACTCAAGGTTTGTGATTCAGATGCCTGTCTGAGGATCTGCCTCATAGCCCTGCTGC.

For human ESC, sgRNA target sequences are as following: *TP53*:gagcgctgctcagatagcga; *TP63*: tttgtcgcaccatcttctga; *TP73*: gcaccacgtttgagcacctc.

Plasmids, lentivirus and chemicals

Lentiviral infections and plasmid transfections were performed as previously described (Xi et al., 2011). The p53^{S212A} and p53^{S212D} plasmids (kindly provided by I. Lemischka), (Lee et al., 2012), Human TAp63α cDNA (Vigene Bioscience, CH842945) and human TAp73α cDNA (kindly provided by E. Flores) were sub-cloned into the pLVX-EF1α-IRES-mCherry vector (Clontech) and a FLAG- or HA- tag was added accordingly. p63 and p73 mutants were generated by site-directed mutagenesis using pairs of mutagenic primers: p63^{S285A}, 5'-cccatcacaggaagacagg<u>c</u>tgtgctggtaccttatga-3'; p63^{S285D}, 5'-cccatcacaggaagacag<u>ga</u>tgtgctggtaccttatga-3'; p73^{S235A}, 5'-caccggcaggcag<u>gc</u>cgtcgtggtgccc-3'; and p73^{S235D}, 5'-caccggcaggcag<u>ga</u>cgtcgtggtgccc-3'. To generate plasmids for doxycycline-inducible vectors of mouse *Wnt3* and *Tcf3*, the ORFs of *Wnt3* (42276,Addgene) and *Tcf3* (kindly provided by H. Nguyen) were cloned into pLVX-Tight-Puro vector (Clontech), separately. In addition, the CMV promoter present in plasmid pLVX-Tet-On was replaced with a pGK promoter to avoid silencing in embryonic stem cells.

Wnt inhibitors IWP-2 (10536, Sigma-Aldrich) and XAV939 (X3004, Sigma-Aldrich) were used at 2.5 μM, and DKK-1 (5439,R&D) at 100ng/ml. SB431542 (Tocris, #1614) was used at 10μM. Recombinant human activin A (R&D Systems, 338-AC) was used at 50ng/ml. Recombinant mouse Wnt3a (R&D Systems, 1324-WN-010) was

used at 150ng/ml. shRNA targeting vectors were obtained from Mission TRC shRNA library (Sigma-Aldrich).

qRT-PCR analysis

For RNA extraction, $2x10^6$ ES or EB cells, or mouse embryos were collected at the indicated times and processed with the PrepEase RNA spin kit (Affymetrix). 500ng total RNA from each sample was used for cDNA synthesis with Transcriptor First Strand cDNA Synthesis Kit (Roche). Quantitative PCR was performed on a ViiA 7 Real-Time PCR System (Life Technologies). *B2m* was used as internal control for calculating relative expression.

Taqman primers used were: Mm00437762_m1 *B2m*, Mm01731290_g1 *Trp53* (all isoforms) Mm00660220_m1 *Trp73* (all isoforms), Mm01263634_g1 *Trp73* (isoform α), Mm01263882_m1 *Trp73* (*ΔNp*73 isoform α&ζ), Mm00495793_m1 *Trp63* (all isoforms), Mm01150797_m1 *Trp63* (isoforms α-γ), Mm01169470_m1 *Trp63* (*ΔNp63* isoforms α-γ)., Hs99999907_m1 *B2m*, Hs01034249_m1 *TP53*, Hs00978340_m1 *TP63* and Hs01056231_m1 *TP73*.

Sequences of synthesized primers used for qRT-PCR assays (designed with mouse genome mm9):

	Forward	Reverse
Gapdh	CTCCACTCACGGCAAATTCA	CGCTCCTGGAAGATGGTGAT
Gsc	TTGCACAGACAGTCGATGCTACT	TCGTTGCTTTCTCGACCCC
Mixl1	CGGTTCTGGATCATCTCTCA A	TACCGAGAACAAGCCAGCAGT
Skil	GACAGGGAGGCCGAGTATG	CCGCTCCTGTCTGAGTTCAT
T (Brachyury)	TCCTCCATGTGCTGAGACTTGT	CCAAGAGCCTGCCACTTTG
Eomes	GCGCATGTTTCCTTTCTTGAG	GGTCGGCCAGAACCACTTC
Foxa2	TACCCAGGGGGCTATGGT	CCCGCTTTGTTCGTGACT
Nanog	TCTTCCTGGTCCCCACAGTTT	GCAAGAATAGTTCTCGGGATGAA
Smad7	GACAGCTCAATTCGGACAACA	CAGTGTGGCGGACTTGATGA
Wnt3	TGGGCCTGTCTTGGACAAA	GCGATGGCATGCACGAA
Axin2	TGACTCTCCTTCCAGATCCCA	TGCCCACACTAGGCTGACA

Sequences of synthesized primers used for qRT-PCR assays (designed with human genome GRCh38/hg38):

	Forward	Reverse
GAPDH	GGAGCCAAACGGGTCATCATCTC	GAGGGGCCATCCACAGTCTTCT
T (BRACHYURY)	ACCCAGTTCATAGCGGTGAC	CCATTGGGAGTACCCAGGTT
FOXA2	GGGAGCGGTGAAGATGGA	TCATGTTGCTCACGGAGGAGTA

EOMES	CGGCCTCTGTGGCTCAAA	AAGGAAACATGCGCCTGC
WNT3	CTTCTAATGGAGCCCCACCT	GAGCCCAGAGATGTGTACTGC

Chromatin immunoprecipitation

For Chromatin Immunoprecipitation (ChIP)-qPCR and ChIP-Seq, mouse ES cells and EBs were collected at indicated time points, from cells that were incubated with human recombinant activin A (AC, 50 ng/ml; R&D Systems) for 2 h or SB431542 (SB, 10μM, Tocris) for 2-4 h, as indicated in each experiment. Cells were cross-linked with 1% formaldehyde (Sigma-Aldrich) at 37°C for 10-15 min and quenched with 0.125 M glycine for 5 min at room temperature. ChIP was performed as previously described (Xi et al., 2011). Samples were incubated with 3–5 μg of antibody bound to 60 μl Dynabeads protein G (Life Technology), then incubated overnight at 4 °C. 1-2% pre-cleared chromatin prior to primary antibody addition was kept as input DNA. Magnetic beads were washed, chromatin was eluted, and reverse cross-linked ChIP DNA was dissolved in 10 mM Tris pH 8.0 buffer for further analysis. For ChIP-qPCR, immunoprecipitated DNA was analyzed by qRT-PCR, and the amplification product was expressed as percentage of the input, or then normalized to the control experiment for each condition. PCR primer pairs used to amplify the unrelated control or promoter regions of indicated genes are listed below. 1) *Gsc* +6kb enhancer: 5'-CTAGGCTCCTAAACCAACAACA-3' (forward) and 5'-CGTCTGACACATCGGTTCATTA-3' (reverse); 2) *Eomes* -10kb enhancer: 5'-GCCCAGCGGGATGTTAAT-3' (forward) and 5'-AGGAGGAGCTATCTGCTAGAC-3' (reverse); 3) *Eomes* +9kb enhancer: 5'-GCTATCTGCAGACGGCTTAAA-3' (forward) and 5'-AAATGACCCTCCCAGCTAGA-3' (reverse); 4) *Foxa2* -37kb enhancer: 5'-AAATGTGTCACCCAAGGCATTT (forward) and 5'-TTACCAGGTCATCAGTCTCAGC-3' (reverse); 5) *Foxa2* -50kb enhancer: 5'-TCCCAAGTGTTCTGTCCTGAAA-3' (forward) and 5'-CAAGGGGAGTCACAGGAAGC-3' (reverse); 6) *Foxa2* -53kb enhancer: 5'-CTCAGGTGGGCAAACAGTATCT-3' (forward) and 5'-AAAATCCCCATCCAAGTCAGCT-3' (reverse); 7) *Wnt3* -1.5kb: 5'-GAGGATCGGGCTAGGAACTCG-3' (forward) and 5'- GTGTAAGGAGAGCAAGGAACTGG-3' (reverse); 8) *Axin2* promoter primers (Yi et al., 2011) were used as reported. Genomic positions of these primers are given relative to the transcription start site (upstream, -; downstream, +). Antibodies used for ChIP were: Smad2/3 (8685S, Cell Signaling Technology), Lef1 (sc-8591X, Santa Cruz Biotechnology), Tcf1 (2203S, Cell signaling), Tcf3 (sc-8635X, Santa Cruz Biotechnology), Tcf4 (sc-8631X, Santa Cruz Biotechnology), HA (11867423001, 3F10, Roche), FLAG (F3165, Sigma-Aldrich), and p53 (P53-505, Leica Biosystems and sc-6243, Santa Cruz).

Immunoblotting and immunoprecipitation

Cell pellets were lysed with RIPA buffer (Cell Signaling) and protein concentrations were determined using the BCA Protein Assay Kit (Pierce). The Nuclear Complex Co-IP Kit (Active Motif) was used for immunoprecipitation. Proteins were separated by SDS-PAGE using Bis-Tris 4-12% gradient polyacrylamide gels in the MOPS buffer system (Life Technologies) and transferred to nitrocellulose membranes (BioRad) according to standard protocols. Membranes were immunoblotted with antibodies against Trim33 (A301-060A-1, Bethyl), Smad2/3 (8685S, Cell Signaling Technology), Smad4 (Ab40759, Abcam), p73 (ab26123, Abcam and sc-7957, Santa Cruz), p63 (sc-25268 and sc-8343, Santa Cruz Biotechnology), p53 (P53-505, Leica Biosystems), Wnt3 (ab52568, Abcam), Nanog (A300-397A, Bethyl Laboratories), Gsc (ab109024, Abcam), Aurka (610938, BD Transduction Laboratories), Nodal (WH0004838M1, Sigma-Aldrich), Tcf3 (sc-8635X, Santa Cruz Biotechnology), HA (11867423001, 3F10, Roche), FLAG (F3165, Sigma-Aldrich), FoxA2 (sc-6554, Santa Cruz Biotechnology), Eomes (ab23345, Abcam) and γ-Tubulin (T6074, Sigma-Aldrich) in Odyssey-TM blocking buffer (LI-COR). Following primary antibody incubation, membranes were washed and probed with IRDye 800CW donkey-anti-mouse IgG (LICOR) or IRDye 680RD goat-anti-rabbit IgG (LI-COR) secondary antibody and imaged using the LI-COR Odyssey system. All western immunoblots were performed independently at least twice. γ-Tubulin was used as a loading control for all experiments.

Immunofluorescence

For immunofluorescence (IF) embryos were fixed in 4% PFA in PBS 20 min at room temperature and then washed with 0.1% Triton in PBS. ISH was performed using antisense riboprobes as previously described (Nowotschin et al.,

2013). Immunofluorescence was carried out as previously described (Nowotschin et al., 2013). Primary antibodies used: FoxA2 (1:100; sc-6554, Santa Cruz and ab108422, Abcam), T (1:100; AF2085, R&D Systems), Eomes (1:500; ab23345, Abcam). Secondary Alexa-Fluor conjugated antibodies (Life Technologies) were used at a dilution of 1:1000. DNA was visualized using Hoechst-33342 (5 μg/mL, Molecular Probes). For cryosections, fixed embryos were taken through a sucrose gradient, embedded in O.C.T. (Tissue-Tek) and sectioned at 12 μm on a cryostat (CM3050S, Leica).

Image data acquisition, processing and quantitation

Wide field images were collected with Zeiss Axiocam MRc/m CCD cameras mounted on a Leica MZ165FC microscope. Laser-scanning confocal images were acquired using a Zeiss LSM880. Raw data were processed using ZEN software (Zeiss) and assembled in Photoshop CS6 (Adobe).

RNA-Seq and data analysis

Total RNA purified from mouse ES cells and EBs was quantified by Ribogreen and quality assessed by Agilent BioAnalyzer 2000. 500ng RNA with integrity number (RIN) > 9.5 from each sample was used for library construction with TruSeq RNA Sample Prep Kit v2 (Illumina) according to manufacturer's instructions. Multiplexed sequencing libraries were run on a Hiseq2500 platform and more than 40million raw paired-end reads were generated for each sample. For data analysis, reads pairs in FASTQ format (50bp/50bp) were quality assessed by FastQC v0.11.3 and mapped to mouse genome mm9 (NCBI build 37, July/2007) with STAR2.3.0e (Dobin et al., 2013) using standard settings for paired reads. On average 82% of raw reads were uniquely mapped. Uniquely mapped reads were counted to each gene with HTSeq v0.5.4 (Ref. 40) with default settings. Read counts were normalized by library size through the "*DESeq2*" (Anders and Huber, 2010; Love et al., 2014) package deposited in Bioconductor. Differential gene expression analysis between any two conditions was performed based on a model utilizing the negative binomial distribution (Anders and Huber, 2010; Love et al., 2014). Genes with FDR<0.05, fold change > 2.0 or < 0.5, and average normalized read counts > 10 were called as differentially expressed genes unless otherwise indicated. Basic statistical calculations were done in R (v3.0.1). Heatmaps for RNA-Seq data were generated with *heatmap.2* function in *gplots* package.

ChIP-Seq and data analysis

For library construction and sequencing, ChIP-Seq DNA samples were quantified and quality assessed by Ribogreen and Agilent Bioanalyzer. DNA fragments range from 200-600bp were selected constructed for ChIP-Seq library with TruSeq ChIP Sample Prep Kit (Illumina) according to manufacturer's instructions. Sequencing libraries were multiplexed and run on a Hiseq 2000 platform.

For mapping and visualization, single end (50bp) or paired-end (50/50bp) FASTQ reads were mapped to mouse genome mm9 (NCBI build 37, Jul/2007) with Bowtie2 with default filtering criteria (Langmead and Salzberg, 2012). Resulted SAM files were converted to BAM files though Samtools 0.1.19 (Li et al., 2009). BAM files were sorted and indexed with Samtools (Li et al., 2009). To visualize ChIP-Seq data, BAM files were converted to TDF file by IGV Tools 2.3.32(Robinson et al., 2011) using the command "igvtools count -z 5 -w 25 -e 250", specifying the coverage window size to be 25bp and average fragment size of 250bp. TDF files were loaded into IGV genome browser (Robinson et al., 2011) and signal intensities normalized by "$1x10^6$/total million reads" or Reads Per Million Reads (RPM) to display normalized coverage data tracks. Scale bars indicating length of genomic ranges is provided above each gene track plot.

Peak calling from ChIP-Seq data was performed with MACS 1.4.2 and verified by HOMER (v4.2) (Heinz et al., 2010). The parameters for peak calling included fold change >8, p value < 1e-8 to detect high confidence binding events. Input samples were used as reference controls for background correction. Peaks identified from MACS 1.14.2 are annotated with HOMER (v4.2) using *annotatePeaks.pl* function. Genes are assigned with the "nearest TSS" criteria. Peak region overlap was performed with the *intersect* function from Bedtools 2.17.0 (Quinlan and Hall, 2010). Conservation data for mammals and vertebrates were extracted from UCSC genome browser and plotted together with ChIP-Seq data tracks. Differentially bound peaks between two conditions were identified by

mergePeaks.pl function in HOMER (v4.2) and validated selectively in the IGV browser. Overlapped peaks were detected by *bed –intersection* tool from bedtools v2.25.0.

Tag density for genomic ranges surrounding defined peak centers were calculated using *annotatePeaks.pl* function in HOMER (v4.2). log2 transformed tag densities were pre-ranked by peak score. Data matrix from each ChIP-Seq experiment were merged by peak names and plotted for heatmaps in R. White indicates low tag density and blue indicates high tag density in each figure.

DNA motif enrichment analysis was performed with HOMER (v4.2) and verified by MEME (Machanick and Bailey, 2011). BED file of Smad2/3 binding peak regions identified by MACS 1.4.2 and HOMER were used as input for HOMER *findMotifs.pl* tool.

For Gene Ontology analysis, genes adjacent to peaks of interest were used as input for the web tool of Gene Ontology (Gene Ontology Consortium) and results were plotted as bar graph with fold change and adjusted p-value.

Statistical analysis

Quantitative data are expressed as mean± s.e.m. Statistical significance was determined using a two-tailed Mann-Whitney test using Prism 6 software (GraphPad Software) unless otherwise indicated.

SUPPLEMENTAL REFERENCES

Anders, S., and Huber, W. (2010). Differential expression analysis for sequence count data. Genome biology *11*, R106.

Carney, K., Chang, Y.M., Wilson, S., Calnan, C., Reddy, P.S., Chan, W.Y., Gilmartin, T., Hernandez, G., Schaffer, L., Head, S.R.*, et al.* (2016). Regulatory T-cell-intrinsic amphiregulin is dispensable for suppressive function. The Journal of allergy and clinical immunology *137*, 1907-1909.

Dobin, A., Davis, C.A., Schlesinger, F., Drenkow, J., Zaleski, C., Jha, S., Batut, P., Chaisson, M., and Gingeras, T.R. (2013). STAR: ultrafast universal RNA-seq aligner. Bioinformatics *29*, 15-21.

Heinz, S., Benner, C., Spann, N., Bertolino, E., Lin, Y.C., Laslo, P., Cheng, J.X., Murre, C., Singh, H., and Glass, C.K. (2010). Simple combinations of lineage-determining transcription factors prime cis-regulatory elements required for macrophage and B cell identities. Molecular cell *38*, 576-589.

Langmead, B., and Salzberg, S.L. (2012). Fast gapped-read alignment with Bowtie 2. Nature methods *9*, 357-359.

Lee, D.F., Su, J., Ang, Y.S., Carvajal-Vergara, X., Mulero-Navarro, S., Pereira, C.F., Gingold, J., Wang, H.L., Zhao, R., Sevilla, A.*, et al.* (2012). Regulation of embryonic and induced pluripotency by aurora kinase-p53 signaling. Cell Stem Cell *11*, 179-194.

Li, H., Handsaker, B., Wysoker, A., Fennell, T., Ruan, J., Homer, N., Marth, G., Abecasis, G., Durbin, R., and Genome Project Data Processing, S. (2009). The Sequence Alignment/Map format and SAMtools. Bioinformatics *25*, 2078-2079.

Li, M., He, Y., Dubois, W., Wu, X., Shi, J., and Huang, J. (2012). Distinct regulatory mechanisms and functions for p53-activated and p53-repressed DNA damage response genes in embryonic stem cells. Molecular cell *46*, 30-42.

Love, M.I., Huber, W., and Anders, S. (2014). Moderated estimation of fold change and dispersion for RNA-seq data with DESeq2. Genome biology *15*, 550.

Machanick, P., and Bailey, T.L. (2011). MEME-ChIP: motif analysis of large DNA datasets. Bioinformatics *27*, 1696-1697.

Ng, E.S., Davis, R., Stanley, E.G., and Elefanty, A.G. (2008). A protocol describing the use of a recombinant protein-based, animal product-free medium (APEL) for human embryonic stem cell differentiation as spin embryoid bodies. Nature protocols *3*, 768-776.

Nowotschin, S., Costello, I., Piliszek, A., Kwon, G.S., Mao, C.A., Klein, W.H., Robertson, E.J., and Hadjantonakis, A.K. (2013). The T-box transcription factor Eomesodermin is essential for AVE induction in the mouse embryo. Genes & development *27*, 997-1002.

Quinlan, A.R., and Hall, I.M. (2010). BEDTools: a flexible suite of utilities for comparing genomic features. Bioinformatics *26*, 841-842.

Robinson, J.T., Thorvaldsdottir, H., Winckler, W., Guttman, M., Lander, E.S., Getz, G., and Mesirov, J.P. (2011). Integrative genomics viewer. Nature biotechnology *29*, 24-26.

Soh, C.L., Giudice, A., Jenny, R.A., Elliott, D.A., Hatzistavrou, T., Micallef, S.J., Kianizad, K., Seach, N., Zuniga-Pflucker, J.C., Chidgey, A.P.*, et al.* (2014). FOXN1 (GFP/w) reporter hESCs enable identification of integrin-beta4, HLA-DR, and EpCAM as markers of human PSC-derived FOXN1(+) thymic epithelial progenitors. Stem cell reports *2*, 925-937.

Xi, Q., Wang, Z., Zaromytidou, A.I., Zhang, X.H., Chow-Tsang, L.F., Liu, J.X., Kim, H., Barlas, A., Manova-Todorova, K., Kaartinen, V.*, et al.* (2011). A poised chromatin platform for TGF-beta access to master regulators. Cell *147*, 1511-1524.

Yi, F., Pereira, L., Hoffman, J.A., Shy, B.R., Yuen, C.M., Liu, D.R., and Merrill, B.J. (2011). Opposing effects of Tcf3 and Tcf1 control Wnt stimulation of embryonic stem cell self-renewal. Nature cell biology *13*, 762-770.

Ying, Q.L., Wray, J., Nichols, J., Batlle-Morera, L., Doble, B., Woodgett, J., Cohen, P., and Smith, A. (2008). The ground state of embryonic stem cell self-renewal. Nature *453*, 519-523.